

Grid-point and time-step requirements for direct numerical simulation and large-eddy simulation

Xiang I. A. Yang (杨翔)^{1, a)} and Kevin P. Griffin²

¹⁾Department of Mechanical Engineering, Pennsylvania State University, State College, PA, 16802, USA

²⁾Center for Turbulence Research, Stanford University, Stanford, CA, 94305, USA

We revisit the grid-point requirement estimates in Choi and Moin [*Phys. Fluid*, **24**, 011702 (2012)] and establish more general grid-point requirements for direct numerical simulations (DNS) and large-eddy simulations (LES) of a spatially developing turbulent boundary layer. We show that, by allowing the local grid spacing to scale with the local Kolmogorov length scale, the grid-point requirement for DNS of a spatially developing turbulent boundary layer is $N \sim Re_{L_x}^{2.05}$ rather than $N \sim Re_{L_x}^{2.64}$ as suggested by Choi and Moin, where N is the number of grid points and L_x is the length of the plate. In addition to the grid-point requirement, we estimate the time-step requirement for DNS and LES. We show that, for a code that treats the convective term explicitly, the time steps required to get converged statistics are $N_t \sim Re_{L_x}/Re_{x_0}^{6/7}$ for wall-modeled LES and $N_t \sim Re_{L_x}/Re_{x_0}^{1/7}$ for wall-resolved LES and DNS (with different prefactors), where Re_{x_0} is the inlet Reynolds number. The grid-point and time-step requirement estimates allow us to estimate the overall cost of DNS and LES. According to present estimates, the costs of DNS, wall-resolved LES and wall-modeled LES scale as $Re_{L_x}^{2.91}$, $Re_{L_x}^{2.72}$, and $Re_{L_x}^{1.14}$.

I. INTRODUCTION

Many fields where computational fluid dynamics (CFD) plays an important role are cost-driven, and therefore, the grid-point and time-step requirements for CFD calculations are important practical issues. The first formal estimate for the grid-point requirement is by Chapman.¹ He estimated the grid-point requirement for wall-resolved large-eddy simulation (WRLES) of a spatially developing turbulent boundary layer and arrived at the estimate $N \sim Re_{L_x}^{9/5}$, where N is the number of grid point, $Re_{L_x} = U_\infty L_x / \nu$ is the Reynolds number, U_∞ is the freestream velocity, L_x is the streamwise length of the flat plate, and ν is the kinematic viscosity. Choi and Moin² revisited Chapman's estimate. By invoking more accurate Reynolds number scalings for the skin friction coefficient and the boundary-layer thickness, Choi and Moin arrived at the estimate $N \sim Re_{L_x}^{2.65}$, $N \sim Re_{L_x}^{1.86}$, and $N \sim Re_{L_x}^1$ for direct numerical simulation (DNS), WRLES, and wall-modeled large-eddy simulation (WMLES), respectively. Rezaeiravesh et al.³ generalized Choi and Moin's estimate by allowing for general Reynolds number scalings for the skin friction and the boundary layer thickness. Liefvendahl and Fureby⁴ followed Rezaeiravesh et al. and estimated the computational cost of ship hull hydrodynamics simulations. The objective of this paper is to revisit the grid-point requirements for DNS, WRLES, and WMLES of a spatially developing turbulent boundary layer and estimate the time-step requirement for DNS, WRLES, and WMLES.

We begin our discussion by pointing out two weak points in the Chapman and Choi & Moin's estimates. In arriving at his estimate, Chapman assumed the use of nested grids, as is sketched in figure 1 (a), where the streamwise, the wall-normal, and the spanwise grid spacings Δx , Δy , and Δz double from block to block. He then concluded that the total number of grid points in the boundary layer is $N = N_1 [1 + 1/4 + (1/4)^2 + (1/4)^3 + \dots] = 4/3 N_1$, giving rise to the coefficient 4/3: the total number of grid points N is 4/3 the number of grid points in the wall layer N_1 . Choi and Moin followed Chapman and invoked the relation $N = 4/3 N_1$.² However, the factor N/N_1 , generally speaking, depends on the grid coarsening from one block to the next. If the grid spacing coarsens by a factor of 1.5, N/N_1 would be 2, leading to arbitrariness in the grid-point estimates. This arbitrariness is the first weak point, and we will try to remove this weak point by allowing the grid spacing to depend on physical length scales. The second weak point in Choi and Moin's analysis is the use of un-nested grids in the wall-normal-spanwise plane for the estimate of the grid-point requirement for DNS.² Figure 1 (b) is a sketch of an un-nested grid: the grid spacing is the same in the wall layer and the outer layer. In a wall-bounded flow, the Kolmogorov length scale η is an increasing function of y , and therefore, the use of un-nested grids is overly conservative (as acknowledged by Choi and Moin). Although Choi and Moin used un-nested grid in the spanwise-wall-normal plane, they did allow the grid spacing to depend on x , which necessarily leads to nested grids in the streamwise direction, as shown in figure 1 (c). In the present work, we will remove the second weak point by allowing nested grid in all three Cartesian directions.

The rest of the paper is organized as follows. In section II of this article, we resolve the aforementioned weaknesses by acknowledging: first, the sizes of energy containing eddies in a turbulent boundary layer scale as their distances from the wall;⁵

^{a)}Electronic mail: xzy48@psu.edu

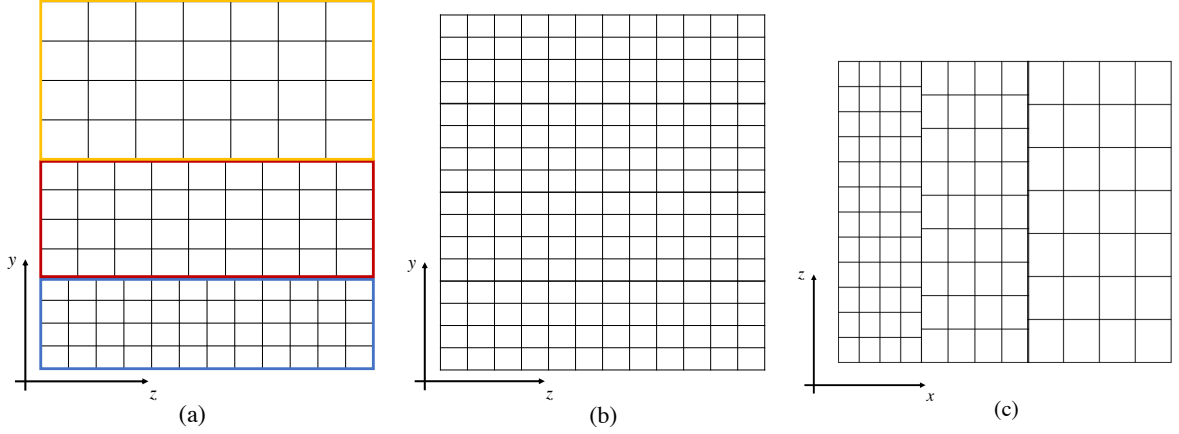


FIG. 1. (a) A sketch of nested grids in a wall-normal/spanwise plane. Three blocks of grids are sketched. Each block contains four layers of grids. The spanwise (and streamwise) grid spacing coarsens from block to block. The first block contains $N_1 = 48$ grid points. The second block contains $N_2 = 36$ grid points. The third block contains $N_3 = 28$ grid points. (b) A sketch of an un-nested grid. (c) A sketch of the assumed streamwise/spanwise grid in Choi and Moin.² The grid spacing depends on x . Here x, y, z are the streamwise, wall-normal, and the spanwise directions.

second, the Kolmogorov length scale is a function of the wall-normal distance. We would follow Choi and Moin and invoke the following relations for the boundary-layer thickness δ and the friction coefficient c_f

$$\begin{aligned} \frac{\delta}{x} &= 0.16 Re_x^{-1/7}, \\ c_f &= 0.027 Re_x^{-1/7}, \end{aligned} \quad (1)$$

which are more accurate for high Reynolds number flows ($10^6 \leq Re_x \leq 10^9$) than the ones used by Chapman.^{6,7} Throughout the article, CM is the abbreviation for Ref. 2. In section III, we estimate the time-step requirements for DNS, WRLES, and WMLES. Concluding remarks are given in section V following a brief discussion in section IV. We include a table of nomenclature in the appendix.

II. GRID-POINT REQUIREMENT

First, we determine the grid-point requirement for a WRLES. While ensuring our derivation is self-contained, we will include references to CM and Chapman as “check points” for validation purposes. These “check points” also help us to highlight the differences between our derivations and the ones in the previous work. The local grid spacing in an LES should be proportional to the sizes of the local energy-containing eddies. In a boundary layer and at a distance above the viscous sublayer, the sizes of the energy containing eddies scale as their distances from the wall. Hence, the grid resolutions are such that $\Delta_x \sim y$, $\Delta_y \sim y$, $\Delta_z \sim y$, which gives rise to

$$\Delta_x = \frac{1}{n_x} y, \quad \Delta_y = \frac{1}{n_y} y, \quad \text{and} \quad \Delta_z = \frac{1}{n_z} y, \quad (2)$$

where $n_x \times n_y \times n_z$ is the number of grid points one deploys in a box of size $y \times y \times y$. The typical values of n_x, n_y and n_z could be found in Ref 2, and we will not repeat these numbers here for brevity. The number of grid points in a box $dx \times dy \times dz$ at a generic location x, y, z is

$$dN_{wr} = \frac{dx}{\Delta_x} \frac{dy}{\Delta_y} \frac{dz}{\Delta_z}. \quad (3)$$

Equation (3) is valid in the wall layer and in the outer layer—thereby, we remove the first weak point in the analysis of CM. Equation (3) directly leads to

$$N_{wr} = \int_V dN_{wr} = N(x < x_0) + \int_{x_0}^{L_x} \frac{dx}{\Delta_{x,w}} \int_0^{L_z} \frac{dz}{\Delta_{z,w}} [N_{y,30}] + \int_{x_0}^{L_x} dx \int_0^{L_z} dz \int_{30v/u_\tau}^{\delta} dy \left[\frac{n_x}{y} \frac{n_y}{y} \frac{n_z}{y} \right], \quad (4)$$

where V is the fluid region, $N(x < x_0)$ is the number of grid points one would need for $x < x_0$, $N_{y,30}$ is the number of y grid points one would need from the wall to $y^+ = 30$, $\Delta_{x,w}$ and $\Delta_{z,w}$ are the grid spacings in the streamwise and the spanwise directions for $y^+ < 30$. To highlight and clarify the variables that are being integrated with respect to, we write first the differentials and their integration limits and second the function to be integrated (a common practice in today's physics/math literature). The second term in Equation (4) is practically equation 12 in CM, but rather than $y^+ = 30$, Choi and Moin used l_y^+ . Following CM, we have

$$\begin{aligned} \int_{x_0}^{L_x} \frac{dx}{\Delta_{x,w}} \int_0^{L_z} \frac{dz}{\Delta_{z,w}} [N_{y,30}] &= L_z N_{y,30} \frac{1}{\Delta_{x,w}^+} \frac{1}{\Delta_{z,w}^+} \int_{x_0}^{L_x} \frac{u_\tau^2}{v^2} dx \\ &= 0.0158 \frac{L_z}{L_x} \frac{N_{y,30}}{\Delta_{x,w}^+ \Delta_{z,w}^+} Re_{L_x}^{13/7} \left[1 - \left(\frac{Re_{x_0}}{Re_{L_x}} \right)^{6/7} \right] \\ &= 0.0158 \frac{L_z}{L_x} \frac{N_{y,30}}{\Delta_{x,w}^+ \Delta_{z,w}^+} \left[Re_{L_x}^{13/7} + O(Re_{L_x}) \right]. \end{aligned} \quad (5)$$

The result in Equation (5) is consistent with equation 13 in CM. This serves as a validation of our derivation. The third term in Equation (4) is

$$\begin{aligned} \int_{x_0}^{L_x} dx \int_0^{L_z} dz \int_{30v/u_\tau}^{\delta} dy \left[\frac{n_x}{y} \frac{n_y}{y} \frac{n_z}{y} \right] &= L_z n_x n_y n_z \int_{x_0}^{L_x} \frac{1}{2} \left(\frac{u_\tau^2}{900v^2} - \frac{1}{\delta^2} \right) dx \\ &= C_1 \frac{L_z}{L_x} n_x n_y n_z \left\{ Re_{L_x}^{13/7} \left[1 - \left(\frac{Re_{x_0}}{Re_{L_x}} \right)^{6/7} \right] + C_2 Re_{L_x}^{2/7} \left[1 - \left(\frac{Re_{L_x}}{Re_{x_0}} \right)^{5/7} \right] \right\} \\ &= C_1 \frac{L_z}{L_x} n_x n_y n_z \left[Re_{L_x}^{13/7} + O(Re_{L_x}) \right], \end{aligned} \quad (6)$$

where $C_1 = 8.75 \times 10^{-6}$ and $C_2 = 27.3/C_1$. In practice, $N_{y,30} \approx n_y$. By definition, $n_x = 30/\Delta_{x,w}^+$ and $n_z = 30/\Delta_{z,w}^+$. Plugging Equations (5) and (6) into Equation (4), we have

$$\begin{aligned} N_{wr} &= \left(0.0158 + 8.75 \times 10^{-6} \times 30^2 \right) \frac{L_z}{L_x} \frac{n_y}{\Delta_{x,w}^+ \Delta_{z,w}^+} Re_{L_x}^{13/7} + O(Re_{L_x}) \\ &= 0.024 \frac{L_z}{L_x} \frac{n_y}{\Delta_{x,w}^+ \Delta_{z,w}^+} Re_{L_x}^{13/7} + O(Re_{L_x}). \end{aligned} \quad (7)$$

The estimate turns out to be only slightly different from that in CM—with the same Reynolds number scaling and with the pre-factor being 0.021 in CM and 0.024 here. Again, the use of nested grids is assumed.

Second, we determine the grid-point requirement for DNS. It follows from Equation (1) that

$$Re_\tau = 0.019 Re_x^{11/14}, \quad (8)$$

for $10^6 < Re_x < 10^9$, or $9.8 \times 10^2 < Re_\tau < 2.2 \times 10^5$. For flows at these high Reynolds numbers,

$$\text{Dissipation} = \varepsilon \approx \text{Production} = -\langle u'v' \rangle \frac{dU}{dy} \approx \frac{u_\tau^3}{\kappa} \frac{1}{y} \quad (9)$$

is a fairly good working approximation of the dissipation in the logarithmic layer, i.e., for $y^+ > 30$, where $\kappa = 0.4$ is the von Karman constant. Figure 2 compares Equation (9) and data at $Re_\tau = 1000, 2000$, and 5200 . It follows from Equation (9) that

the Kolmogorov length scale is

$$\eta = \left(\frac{v^3}{\varepsilon} \right)^{1/4} \sim \left(\frac{v}{u_\tau} \right)^{3/4} y^{1/4}, \quad (10)$$

for $y^+ > 30$, where ε is the total dissipation. For $y^+ < 30$, a conservative estimate of the dissipation rate is $\varepsilon^+ = 1$,² and a conservative estimate of the Kolmogorov length scale follows: $\eta^+ = 1$. The grid resolution in a DNS is proportional to the local Kolmogorov length scale, i.e.,

$$\Delta_x = C_x \eta, \quad \Delta_y = C_y \eta, \quad \text{and} \quad \Delta_z = C_z \eta, \quad (11)$$

where C_x , C_y , and C_z are $O(1)$ constants. Hence, the number of grid points needed for a DNS of a spatially developing boundary layer is

$$\begin{aligned} N_{DNS} = \int_V \frac{dx}{\Delta_x} \frac{dy}{\Delta_y} \frac{dz}{\Delta_z} = & N(x < x_0) + \int_{x_0}^{L_x} \frac{dx^+}{C_x} \int_0^{L_z} \frac{dz^+}{C_z} \frac{30}{C_y} \\ & + \int_{x_0}^{L_x} dx \int_0^{L_z} dz \int_{30v/u_\tau}^{\delta} dy \left[\frac{1}{C_x C_y C_z} \left(\frac{v}{u_\tau} \right)^{-9/4} \frac{1}{y^{3/4}} \right]. \end{aligned} \quad (12)$$

A 9/4 exponent emerges as expected. This 9/4 gives rise to the $N_{DNS} \sim Re^{9/4}$ in Ref 8. The second term in Equation (12) is

$$\begin{aligned} \int_{x_0}^{L_x} \frac{dx^+}{C_x} \int_0^{L_z} \frac{dz^+}{C_z} \frac{30}{C_y} &= L_z \frac{1}{C_x C_y C_z} \frac{30}{v^2} \int_{x_0}^{L_x} u_\tau^2 dx \\ &= 0.473 \frac{L_z}{L_x} \frac{1}{C_x C_y C_z} Re_{L_x}^{13/7} \left[1 - \left(\frac{Re_{x_0}}{Re_{L_x}} \right)^{6/7} \right] \\ &= 0.473 \frac{L_z}{L_x} \frac{1}{C_x C_y C_z} Re_{L_x}^{13/7} + O(Re_{L_x}). \end{aligned} \quad (13)$$

The third term in Equation (12) is

$$\begin{aligned} & \int_{x_0}^{L_x} dx \int_0^{L_z} dz \int_{30v/u_\tau}^{\delta} dy \left[\frac{1}{C_x C_y C_z} \left(\frac{v}{u_\tau} \right)^{-9/4} \frac{1}{y^{3/4}} \right] \\ &= \frac{1}{C_x C_y C_z} \frac{1}{v^{9/4}} L_z \int_{x_0}^{L_x} 4u_\tau^{9/4} \left[\delta^{1/4} - (30v/u_\tau)^{1/4} \right] dx \\ &= \frac{0.019}{C_x C_y C_z} \frac{L_z}{L_x} Re_{L_x}^{115/56} \left[1 - \left(\frac{Re_{x_0}}{Re_{L_x}} \right)^{59/56} \right] - \frac{0.15}{C_x C_y C_z} \frac{L_z}{L_x} Re_{L_x}^{13/7} \left[1 - \left(\frac{Re_{x_0}}{Re_{L_x}} \right)^{6/7} \right] \\ &= 0.019 \frac{1}{C_x C_y C_z} \frac{L_z}{L_x} Re_{L_x}^{115/56} + O(Re_{L_x}^{13/7}). \end{aligned} \quad (14)$$

Plugging Equations (13) and (14) into Equation (12), we have

$$N_{DNS} = 0.019 \frac{1}{C_x C_y C_z} \frac{L_z}{L_x} Re_{L_x}^{115/56} + O(Re_{L_x}^{13/7}). \quad (15)$$

Compared to the estimate in CM, i.e., $N_{DNS} \sim Re_{L_x}^{37/14}$, the estimate in Equation (15) indicates a much weaker dependence on Re_{L_x} due to the use of a nested grid. In arriving at Equation (15), we assume $\varepsilon \sim 1/y$ above $y^+ = 30$. As shown in figure 2, this overestimates the dissipation rate in the wake layer, which in turn leads to an underestimate of the Kolmogorov length scale and a conservative estimate of the grid-point requirement.

Next, we compare the grid-point requirements of WMLES, WRLES, and DNS. By assuming that the grid spacing scales as the local boundary layer height δ and that the LES/wall-model matching location is at some fraction of δ (most wall models should have no difficulty complying with this requirement^{12–22}), Choi and Moin concluded that $N_{wm} \sim Re_{L_x}^1$. In all, to resolve a spatially developing turbulent boundary layer, a WMLES requires $N_{wm} \sim Re_{L_x}^{1.00}$, a WRLES requires $N_{wr} \sim Re_{L_x}^{13/7} = Re_{L_x}^{1.86}$, and a DNS requires $N_{DNS} \sim Re_{L_x}^{115/56} = Re_{L_x}^{2.05}$.

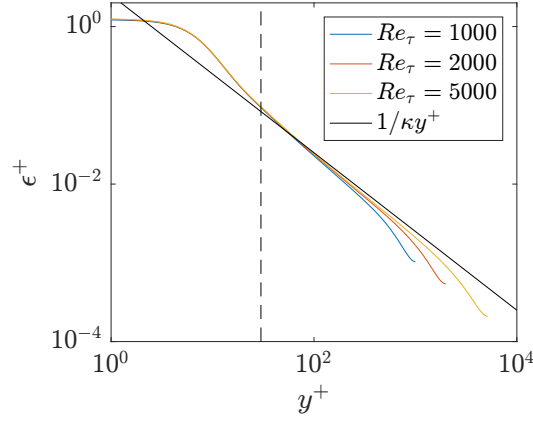


FIG. 2. Dissipation rate in channel flow at $Re_\tau = 1000, 2000$, and 5200 . Details of the data could be found in Refs. 9–11. Here, ε is the total dissipation, and it includes $\nu(dU/dy)^2$. The superscript $+$ denotes normalization by wall units.

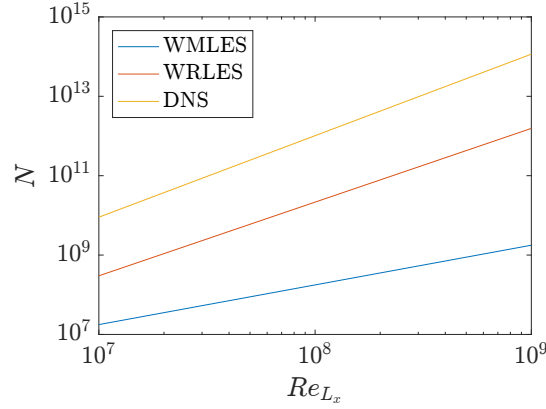


FIG. 3. Number of grid points needed for DNS, WRLES, and WMLES of a spatially developing turbulent boundary layer.

Figure 3 shows the number of grid points for WMLES, WRLES, and DNS of a spatially developing turbulent boundary layer as a function of Re_{L_x} . The grid-point requirement for WMLES is

$$N_{wm} = 54.7 \frac{L_z}{L_x} n_x n_y n_z Re_{L_x}^{2/7} \left[\left(\frac{Re_{L_x}}{Re_{x_0}} \right)^{5/7} - 1 \right], \quad (16)$$

following Ref 2. When generating this figure, we have followed Choi and Moin and assume $Re_{x_0} = 5 \times 10^5$, $n_x n_y n_z = 2500$, $n_y/\Delta_{w,x}^+ \Delta_{w,z}^+ = 1/200$, and $L_x/L_z = 4$. The constants $C_x C_y C_z = 125$. We neglect the grid points needed for $x < x_0$ and retained only the leading order term. As a result, the estimates are only valid for $Re_{L_x} \gg Re_{x_0}$. According to figure 3, in this Reynolds number range, DNS is about 100 times more costly than WRLES. If the computing ability doubles every two years, i.e., if Moore's (or Koomey's²³) law holds, the Reynolds number range that is accessible to WRLES today will be accessible to DNS in about 13 years. In addition, compared with WRLES, WMLES becomes increasingly more cost-efficient as the Reynolds number increases.^{24,25}

III. TIME-STEP REQUIREMENT

The cost of a simulation is a direct function of the time-step requirement. In this section, we estimate the number of time steps required to get converged statistics. Mathematically,

$$\text{Time step requirement} = \frac{\text{Physical time needed for converged statistics}}{\text{Time step size}}. \quad (17)$$

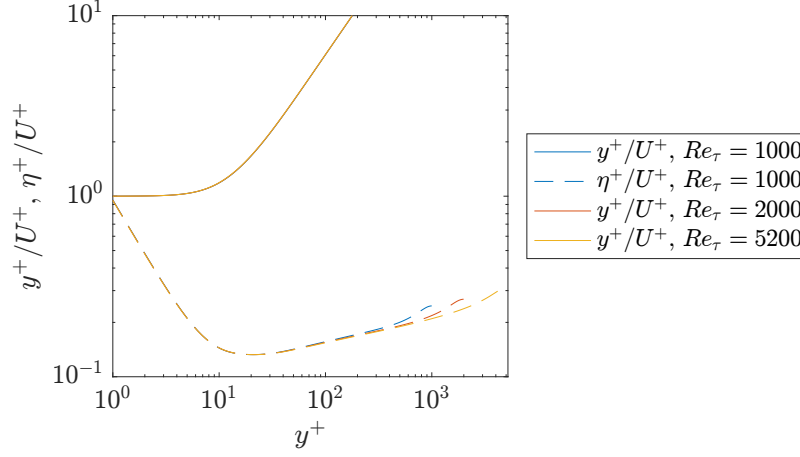


FIG. 4. y^+/U^+ and η^+/U^+ as a function of the wall-normal distance in a channel at Reynolds numbers $Re_\tau = 1000, 2000$, and 5200 . Solid lines are for y^+/U^+ . Dashed lines are for η^+/U^+ . Different Reynolds numbers are color-coded, with blue for $Re_\tau = 1000$, red for $Re_\tau = 2000$, yellow for $Re_\tau = 5200$.

We first estimate the time step size, dt . If one treats both the viscous term and the convective term implicitly, there is no stability requirement for the time step size. A more common practice is to treat the viscous term implicitly and the convective term explicitly.^{26–28} For these semi-implicit codes, the Courant–Friedrichs–Lewy (CFL) number has to be smaller than some $\mathcal{O}(1)$ value. For an incompressible flow solver, an estimate of the local CFL number is

$$\begin{aligned} \text{CFL} &= \frac{U dt}{\Delta_x} = \frac{u_\tau^2 dt}{\nu} \frac{U^+}{\delta^+/n_x}, \quad \text{for WMLES;} \\ &= \frac{u_\tau^2 dt}{\nu} \frac{U^+}{y^+/n_x}, \quad \text{for WRLES;} \\ &= \frac{u_\tau^2 dt}{\nu} \frac{U^+}{C_x \eta^+}, \quad \text{for DNS,} \end{aligned} \quad (18)$$

where we neglect fluctuations in the velocity (the root mean square of U is small compared to U itself). For the purpose of this discussion, we require $\text{CFL} \leq 1$, and it follows from Equation (18) that

$$\begin{aligned} dt &\leq \min_{x,y} \left[\frac{\nu}{u_\tau^2} \frac{\delta^+/n_x}{U^+} \right], \quad \text{for WMLES;} \\ dt &\leq \min_{x,y} \left[\frac{\nu}{u_\tau^2} \frac{y^+/n_x}{U^+} \right], \quad \text{for WRLES;} \\ dt &\leq \min_{x,y} \left[\frac{\nu}{u_\tau^2} \frac{C_x \eta^+}{U^+} \right], \quad \text{for DNS,} \end{aligned} \quad (19)$$

where U^+ and η^+ are functions of y^+ ; u_τ and δ are functions of x ; n_x and C_x are constants. Figure 4 shows y^+/U^+ and η^+/U^+ as a function of y^+ for channel flow at $Re_\tau = 1000, 2000$, and 5200 . According to figure 4, y^+/U^+ attains its minimum, i.e., 1, at $y^+ = 1$, and η^+/U^+ attains its minimum, i.e., 0.13, at $y^+ \approx 15$. Hence, Equation (19) reduces to

$$\begin{aligned} dt &\leq \min_x \left[\frac{\nu}{u_\tau^2} \frac{\delta^+/n_x}{U_\infty^+} \right], \quad \text{for WMLES;} \\ dt &\leq \min_x \left[\frac{\nu}{n_x u_\tau^2} \right], \quad \text{for WRLES;} \\ dt &\leq \min_x \left[0.13 \frac{C_x \nu}{u_\tau^2} \right], \quad \text{for DNS.} \end{aligned} \quad (20)$$

Plugging Equation (1) into Equation (20) leads to

$$\begin{aligned}\frac{U_\infty^2 dt}{\nu} &\leq \min_x \left[\frac{Re_x^{6/7}}{n_x} \right] = \frac{Re_{x_0}^{6/7}}{n_x}, & \text{for WMLES;} \\ \frac{U_\infty^2 dt}{\nu} &\leq \min_x \left[\frac{74}{n_x} Re_x^{1/7} \right] = \frac{74}{n_x} Re_{x_0}^{1/7}, & \text{for WRLES;} \\ \frac{U_\infty^2 dt}{\nu} &\leq \min_x \left[9.6 C_x Re_x^{1/7} \right] = 9.6 C_x Re_{x_0}^{1/7}, & \text{for DNS;}\end{aligned}\tag{21}$$

assuming that the inlet is at $x = x_0$. Near the wall, i.e., at the y locations where y^+/U^+ and η^+/U^+ attain their minimums, typical values are $C_x = 1$, $n_x = 1$, and Equation (21) leads to

$$\begin{aligned}\frac{U_\infty^2 dt}{\nu} &\leq 0.2 Re_{x_0}^{6/7}, & \text{for WMLES;} \\ \frac{U_\infty^2 dt}{\nu} &\leq 74 Re_{x_0}^{1/7}, & \text{for WRLES;} \\ \frac{U_\infty^2 dt}{\nu} &\leq 9.6 Re_{x_0}^{1/7}, & \text{for DNS.}\end{aligned}\tag{22}$$

Next, we estimate the physical time needed to get converged statistics. There are two important simulation time scales: the flow-through time $T_{ft} = L_x/U_\infty$ and the eddy-turn-over time $T_{eto} = \delta/u_\tau$. The flow-through time is associated with the transients of the simulation and the eddy-turn-over time is associated with statistical convergence of turbulence quantities. In order to get converged statistics, one needs to integrate for several (the exact number ranges from less than one hundred to more than two thousand^{29,30}) eddy-turnover times. Using Equation (1),

$$T_{eto} = \frac{\delta}{u_\tau} \Big|_{x=L_x} = 1.38 Re_{L_x}^{13/14} \frac{\nu}{U_\infty^2},\tag{23}$$

and

$$T_{ft} = \frac{L_x}{U_\infty} = Re_{L_x} \frac{\nu}{U_\infty^2}.\tag{24}$$

The flow-through time is slightly larger than the eddy-turn-over time for large Re_{L_x} . We will be conservative and assume that a constant number C_t of flow-through times T_{ft} must be integrated. This implies

$$N_t = C_t T_{ft} / dt = C_t Re_{L_x} \frac{U_\infty^2 dt}{\nu}.\tag{25}$$

It follows from Equations (22) and (25) that

$$\begin{aligned}N_t &= C_t \frac{Re_{L_x}}{0.2 Re_{x_0}^{6/7}}, & \text{for WMLES;} \\ N_t &= C_t \frac{Re_{L_x}}{74 Re_{x_0}^{1/7}}, & \text{for WRLES;} \\ N_t &= C_t \frac{Re_{L_x}}{9.6 Re_{x_0}^{1/7}}, & \text{for DNS.}\end{aligned}\tag{26}$$

Equation (26) is the time-step requirement for DNS, WRLES, and WMLES. Nonetheless, it would be more instructive if we can write these time step estimates in terms of a single Reynolds number. To do that, we need to estimate L_x/x_0 . We consider two common applications. First, in a canonical simulation of the turbulent section of a boundary layer, the domain is usually constructed such that $L_x - x_0 = C_\delta \delta_{L_x}$, where C_δ is a constant (e.g. $C_\delta = 24$ was used in Ref 29). This choice combined with the correlations in Equation (1) imply

$$\frac{x_0}{L_x} = 1 - 0.16 C_\delta Re_{L_x}^{-1/7}.\tag{27}$$

In the high-Reynolds-number limit, $x_0/L_x \rightarrow 1$. Second, we consider the simulation of an airfoil where the transition location is geometrically imposed. Similar to the first case, this implies x_0/L_x is approximately constant. For both of these cases, Equation (26) becomes

$$\begin{aligned} N_t &\sim Re_{L_x}^{1/7}, & \text{for WMLES;} \\ N_t &\sim Re_{L_x}^{6/7}, & \text{for WRLES;} \\ N_t &\sim Re_{L_x}^{6/7}, & \text{for DNS.} \end{aligned} \tag{28}$$

IV. DISCUSSION

Reynolds³¹ proposed a back-of-the-envelope estimate for the time-step requirement. He assumed a constant velocity in the computational domain and argued that the number of time steps N_t scales as $N_t \sim N^{1/3}$, which leads to $N_t \sim Re_{L_x}^{115/168}$ for DNS, $N_t \sim Re_{L_x}^{13/21}$ for WRLES, and $N_t \sim Re_{L_x}^{1/3}$ for WMLES. These estimates for DNS ($N_t \sim Re_{L_x}^{0.68}$) and WRLES ($N_t \sim Re_{L_x}^{0.62}$) are slightly more optimistic than our predictions in Equation (28) ($N_t \sim Re_{L_x}^{0.86}$). Whereas for WMLES, the estimate of Reynolds ($N_t \sim Re_{L_x}^{0.33}$) is more pessimistic than our prediction ($N_t \sim Re_{L_x}^{0.14}$).

A crude estimate for the overall cost of a simulation on a single CPU scales with the number of grid points times the number of time steps, i.e., NN_t . However, provided access to very large computational resources and ideal software parallelization, the wall-clock time required for a simulation scales with N_t only. For this reason, Equation (28) provides a very optimistic outlook for WMLES in the age of exascale computing.

In section III, we have considered only the CFL condition. If one treats the viscous term explicitly, he/she must account for the viscous stability condition:

$$\text{viscous stability condition} = \frac{v dt}{\Delta^2} = \frac{u_\tau^2 dt}{v} \frac{1}{\Delta^{+2}} \leq 1 \tag{29}$$

where Δ is the grid spacing. If a nested grid like the one in figure 1 (a) is used, the grid is locally isotropic, and therefore one could use Δ in any of the three directions for an estimate of the viscous stability condition. For typical boundary layer flow simulations, Δ attains its minimum at the wall, i.e., $\min[\Delta^+] = \Delta_y^+|_{y=0} = O(1)$. It then follows from Equation (29) that

$$dt \leq \min_x \left[\frac{v}{u_\tau^2} \right], \text{ for WRLES and DNS.} \tag{30}$$

Invoking Equation (1), we have

$$\frac{U_\infty^2 dt}{v} \leq 74 Re_{x_0}^{1/7}, \text{ for WRLES and DNS.} \tag{31}$$

For WMLES, because the wall layer is not resolved, the viscous stability condition is not a concern. Comparing Equation (31) with Equation (22), the time steps required to resolve the convective and diffusive physical time scales have the same asymptotic dependence on Reynolds number. An implication of this result is that implicit treatment of the viscous terms typically only leads to a computational speedup by a constant factor.

V. CONCLUSION

The estimates for the grid-point and time-step requirements for DNS, WRLES, and WMLES are summarized in Table I. These estimates depend critically on how one deploys the grid points. Choi & Moin assumed that dx , dy , and dz scales with the Kolmogorov length scale at the wall, and they concluded $N_{\text{DNS}} \sim Re_{L_x}^{2.65}$. Here, by allowing dx , dy , and dz to depend on the local Kolmogorov length scale, we arrive at $N_{\text{DNS}} \sim Re_{L_x}^{2.06}$. Hence, the use of nested grids is critical to the efficient use of the limited computational resources. However, the more common practice is to keep dx and dz constant and vary dy as a function of the wall-normal coordinate,^{11,32–35} which is an inefficient use of the computational resources. While there are other meshing techniques,^{36,37} Voronoi mesh is a promising path to nested grids.^{38,39} One can build a nested Voronoi mesh by clustering points

TABLE I. A summary of Reynolds number scalings of the present and prior grid-point requirements, time-step requirements, and the overall simulation cost. Here, we assume x_0/L_x is Reynolds number independent (see Section III for detailed discussion). * Chapman and Choi & Moin did not formally estimate the time-step requirements; therefore, the estimates of the overall cost are made using the conventional back-of-the-envelope calculation in Refs 31 and 42, i.e., $N_t \sim N^{1/3}$.

	Grid-point exponent a , where $N \sim Re_{L_x}^a$			Time-step exponent b , where $N_t \sim Re_{L_x}^b$			Overall cost exponent c , where $NN_t \sim Re_{L_x}^c$		
	DNS	WRLES	WMLES	DNS	WRLES	WMLES	DNS	WRLES	WMLES
Chapman ¹	-	1.8	0.4	-	-	-	-	2.4*	0.53*
Choi & Moin ²	2.64	1.86	1.0	-	-	-	3.52*	2.48*	1.33*
Present	2.05	1.86	1.0	6/7	6/7	1/7	2.91	2.72	1.14

according to the local grid-point requirement and creating a Voronoi diagram from these scattered points, see, Refs 40 and 41 for recent applications of this technique.

In addition to the grid-point requirements, we estimate the time-step requirements for WMLES, WRLES, and DNS. For a fully explicit or a semi-implicit code, the time-step requirement is $N_t \sim Re_{L_x}/Re_{x_0}^{1/7}$ for DNS, $N_t \sim Re_{L_x}/Re_{x_0}^{1/7}$ for WRLES, $N_t \sim Re_{L_x}/Re_{x_0}^{6/7}$ for WMLES, as shown in Equation (26). Since parallelizing time is very difficult, this estimate provides an optimistic outlook for WMLES. In arriving at the above estimates for the time-step requirements, we obtain two useful conclusions: first, implicit treatment of viscous terms does not significantly benefit time stepping, and second, the most limiting region in terms of time stepping is the buffer layer for DNS rather than the viscous sublayer. Both conclusions, however, are true only if the grid is such that dx , dy , and dz scale with the local Kolmogorov length scale. In practice, dx and dy may be such that $dx^+/dy^+ = \mathcal{O}(10 - 100)$ in the wall layer.^{11,33} In that case, implicit treatment of the viscous term would benefit time stepping.

According to the previous estimates (in Ref 2) and the numbers in the last column of Table I, the saving in the computational cost by going from DNS to WRLES is nearly as significant as from WRLES to WMLES. Because of this prior estimate, WRLES is often perceived as a cost-effective alternative to DNS. The present estimate conveys a very different message. According to the present estimate and the numbers in Table I, if one uses a nested grid and a semi-implicit code, the saving in the computational cost by going from DNS to WRLES is much smaller than that by going from WRLES to WMLES, making WRLES, a computational tool that relies on sub-grid scale modeling, much less attractive. Considering that DNS of flows at practically relevant Reynolds numbers is not going to be possible in the near future, the present estimates give a very promising outlook for WMLES.

ACKNOWLEDGEMENT

XY acknowledges financial support from the Elliott Group and the Office of Naval Research. KG acknowledges support from the National Defense Science and Engineering Graduate Fellowship and the Stanford Graduate Fellowship. XY and KG thank Parviz Moin, Ugo Piomelli, Adrian Lozano-Duran and Vishal Jariwala for their useful comments.

DATA AVAILABILITY

The data that support the findings of this study are available from the corresponding author upon reasonable request.

Appendix A: Nomenclature

In this appendix, we list the variables used in our manuscript.

- C Constant
- c_f friction coefficient
- dt time step size
- L length
- N total number of grid points
- n constant describing WRLES resolution

N_t	number of time steps
Re	Reynolds number
T	time scale
U	mean streamwise velocity
U_∞	freestream velocity
u_τ	friction velocity
u'	streamwise velocity fluctuation
v'	wall-normal velocity fluctuation
x	streamwise coordinate
x_0	inlet location
y	wall-normal coordinate
z	spanwise coordinate

Greek letters

δ	boundary layer thickness
Δ	grid spacing
ε	turbulent dissipation
κ	von Karman constant
η	Kolmogorov length scale
ν	kinematic viscosity

Subscripts

w	wall
wr	wall resolved
eto	eddy turnover
ft	flow through

REFERENCES

- ¹D. R. Chapman, “Computational aerodynamics development and outlook,” *AIAA J.*, vol. 17, no. 12, pp. 1293–1313, 1979.
- ²H. Choi and P. Moin, “Grid-point requirements for large eddy simulation: Chapman’s estimates revisited,” *Phys. Fluids*, vol. 24, no. 1, p. 011702, 2012.
- ³S. Rezaeiravesh, M. Liefvendahl, and C. Fureby, “On grid resolution requirements for les of wall-bounded flows,” 2016.
- ⁴M. Liefvendahl and C. Fureby, “Grid requirements for les of ship hydrodynamics in model and full scale,” *Ocean Engineering*, vol. 143, pp. 259–268, 2017.
- ⁵I. Marusic and J. P. Monty, “Attached eddy model of wall turbulence,” *Ann. Rev. Fluid Mech.*, vol. 51, pp. 49–74, 2019.
- ⁶H. M. Nagib, K. A. Chauhan, and P. A. Monkewitz, “Approach to an asymptotic state for zero pressure gradient turbulent boundary layers,” *Philosophical Transactions of the Royal Society A*, vol. 365, no. 1852, pp. 755–770, 2007.
- ⁷P. A. Monkewitz, K. A. Chauhan, and H. M. Nagib, “Self-consistent high-reynolds-number asymptotics for zero-pressure-gradient turbulent boundary layers,” *Phys. Fluids*, vol. 19, no. 11, p. 115101, 2007.
- ⁸R. S. Rogallo and P. Moin, “Numerical simulation of turbulent flows,” *Ann. Rev. Fluid Mech.*, vol. 16, no. 1, pp. 99–137, 1984.
- ⁹J. Graham, K. Kanov, X. Yang, M. Lee, N. Malaya, C. Lalescu, R. Burns, G. Eyink, A. Szalay, R. Moser, *et al.*, “A web services accessible database of turbulent channel flow and its use for testing a new integral wall model for les,” *J. Turbul.*, vol. 17, no. 2, pp. 181–215, 2016.
- ¹⁰S. Hoyas and J. Jiménez, “Scaling of the velocity fluctuations in turbulent channels up to $Re_\tau = 2003$,” *Phys. Fluids*, vol. 18, no. 1, p. 011702, 2006.
- ¹¹M. Lee and R. D. Moser, “Direct numerical simulation of turbulent channel flow up to $Re_\tau = 5200$,” *J. Fluid Mech.*, vol. 774, pp. 395–415, 2015.
- ¹²S. Kawai and J. Larsson, “Wall-modeling in large eddy simulation: Length scales, grid resolution, and accuracy,” *Phys. Fluids*, vol. 24, no. 1, p. 015105, 2012.
- ¹³G. I. Park and P. Moin, “An improved dynamic non-equilibrium wall-model for large eddy simulation,” *Phys. Fluids*, vol. 26, no. 1, pp. 37–48, 2014.
- ¹⁴S. T. Bose and P. Moin, “A dynamic slip boundary condition for wall-modeled large-eddy simulation,” *Phys. Fluids*, vol. 26, no. 1, p. 015104, 2014.
- ¹⁵X. I. A. Yang, J. Sadique, R. Mittal, and C. Meneveau, “Integral wall model for large eddy simulations of wall-bounded turbulent flows,” *Phys. Fluids*, vol. 27, no. 2, p. 025112, 2015.
- ¹⁶X. I. Yang and Y. Lv, “A semi-locally scaled eddy viscosity formulation for les wall models and flows at high speeds,” *Theoretical and Computational Fluid Dynamics*, vol. 32, no. 5, pp. 617–627, 2018.
- ¹⁷X. I. A. Yang, S. Zafar, J.-X. Wang, and H. Xiao, “Predictive large-eddy-simulation wall modeling via physics-informed neural networks,” *Phys. Rev. Fluids*, vol. 4, no. 3, p. 034602, 2019.
- ¹⁸X. L. Huang, X. I. Yang, and R. F. Kunz, “Wall-modeled large-eddy simulations of spanwise rotating turbulent channels—comparing a physics-based approach and a data-based approach,” *Physics of Fluids*, vol. 31, no. 12, p. 125105, 2019.

- ¹⁹P. S. Iyer and M. R. Malik, "Analysis of the equilibrium wall model for high-speed turbulent flows," *Physical Review Fluids*, vol. 4, no. 7, p. 074604, 2019.
- ²⁰H. J. Bae, A. Lozano-Durán, S. T. Bose, and P. Moin, "Dynamic slip wall model for large-eddy simulation," *J. Fluid Mech.*, vol. 859, pp. 400–432, 2019.
- ²¹C. Meneveau, "A note on fitting a generalised moody diagram for wall modelled large-eddy simulations," *J. Turbul.*, pp. 1–24, 2020.
- ²²K. P. Griffin and L. Fu, "A new ode-based turbulence wall model accounting for pressure gradient and reynolds number effects," *arXiv preprint arXiv:2010.04097*, 2020.
- ²³J. Koomey, S. Berard, M. Sanchez, and H. Wong, "Implications of historical trends in the electrical efficiency of computing," *IEEE Annals of the History of Computing*, vol. 33, no. 3, pp. 46–54, 2011.
- ²⁴J. Larsson, S. Kawai, J. Bodart, and I. Bermejo-Moreno, "Large eddy simulation with modeled wall-stress: recent progress and future directions," *Mech. Eng. Rev.*, vol. 3, no. 1, pp. 15–00418, 2016.
- ²⁵S. T. Bose and G. I. Park, "Wall-modeled large-eddy simulation for complex turbulent flows," *Ann. Rev. Fluid Mech.*, vol. 50, pp. 535–561, 2018.
- ²⁶R. Mittal, H. Dong, M. Bozkurtas, F. Najjar, A. Vargas, and A. Von Loebbecke, "A versatile sharp interface immersed boundary method for incompressible flows with complex boundaries," *J Comput Phys*, vol. 227, no. 10, pp. 4825–4852, 2008.
- ²⁷C. Scalo, J. Bodart, and S. K. Lele, "Compressible turbulent channel flow with impedance boundary conditions," *Phys. Fluids*, vol. 27, no. 3, p. 035107, 2015.
- ²⁸I. Bermejo-Moreno, L. Campo, J. Larsson, J. Bodart, D. Helmer, and J. K. Eaton, "Confinement effects in shock wave/turbulent boundary layer interactions through wall-modelled large-eddy simulations," *Journal of Fluid Mechanics*, vol. 758, p. 5, 2014.
- ²⁹T. S. Lund, X. Wu, and K. D. Squires, "Generation of turbulent inflow data for spatially-developing boundary layer simulations," *J Comput Phys*, vol. 140, no. 2, pp. 233–258, 1998.
- ³⁰S. Leonardi and I. P. Castro, "Channel flow over large cube roughness: a direct numerical simulation study," *J. Fluid Mech.*, vol. 651, pp. 519–539, 2010.
- ³¹W. C. Reynolds, "The potential and limitations of direct and large eddy simulations," in *Whither turbulence? Turbulence at the crossroads*, pp. 313–343, Springer, 1990.
- ³²J. Kim, P. Moin, and R. Moser, "Turbulence statistics in fully developed channel flow at low reynolds number," *J. Fluid Mech.*, vol. 177, pp. 133–166, 1987.
- ³³A. Lozano-Durán and J. Jiménez, "Effect of the computational domain on direct simulations of turbulent channels up to $Re_\tau = 4200$," *Phys. Fluids*, vol. 26, no. 1, p. 011702, 2014.
- ³⁴J. Ryu, S. G. Park, W.-X. Huang, and H. J. Sung, "Hydrodynamics of a three-dimensional self-propelled flexible plate," *Phys. Fluids*, vol. 31, no. 2, p. 021902, 2019.
- ³⁵Y.-J. Dai, W.-X. Huang, and C.-X. Xu, "Coherent structures in streamwise rotating channel flow," *Phys. Fluids*, vol. 31, no. 2, p. 021204, 2019.
- ³⁶A. Kravchenko, P. Moin, and R. Moser, "Zonal embedded grids for numerical simulations of wall-bounded turbulent flows," *J Comput Phys*, vol. 127, no. 2, pp. 412–423, 1996.
- ³⁷S. Toosi and J. Larsson, "Anisotropic grid-adaptation in large eddy simulations," *Computers & Fluids*, vol. 156, pp. 146–161, 2017.
- ³⁸G. Voronoi, "New parametric applications concerning the theory of quadratic forms-second announcement," *J. Reine Angew. Math.*, vol. 134, pp. 198–287, 1908.
- ³⁹J. M. Augenbaum and C. S. Peskin, "On the construction of the voronoi mesh on a sphere," *J Comput Phys*, vol. 59, no. 2, pp. 177–192, 1985.
- ⁴⁰O. Lehmkuhl, G. Park, S. Bose, and P. Moin, "Large-eddy simulation of practical aeronautical flows at stall conditions," *Proceedings of the 2016 Summer Program, Center for Turbulence Research, Stanford University*, 2018.
- ⁴¹K. Goc, S. Bose, and P. Moin, "Wall-modeled large eddy simulation of an aircraft in landing configuration," in *AIAA AVIATION 2020 FORUM*, p. 3002, 2020.
- ⁴²U. Piomelli and E. Balaras, "Wall-layer models for large-eddy simulations," *Ann. Rev. Fluid Mech.*, vol. 34, no. 1, pp. 349–374, 2002.